University of Groningen

Machine-perfused donor kidneys as a source of human renal endothelial cells

COMBAT Consortium; Lammerts, Rosa Geerlinde Margriet; Lagendijk, Lisanne M; Tiller, Gesa; Dam, Wendy A; Lancaster, Harriet L; Daha, Mohamed R; Seelen, Marc A; Hepkema, Bouke G; Pol, Robert A

IMPORTANT NOTE: You are advised to consult the publisher's version (publisher's PDF) if you wish to cite from it. Please check the document version below.

Document Version
Publisher's PDF, also known as Version of record

[Link to publication in University of Groningen/UMCG research database](#)

RESEARCH ARTICLE

Translational Physiology

Machine-perfused donor kidneys as a source of human renal endothelial cells

Rosa G. M. Lammerts,[1] Lisanne M. Lagendijk,[1] Gesa Tiller,[1] Wendy A. Dam,[1] Harriet L. Lancaster,[1] Mohamed R. Daha,[1] Marc A. Seelen,[1] Bouke G. Hepkema,[3] Robert A. Pol,[2] Henri G. D. Leuvenink,[2] Grietje Molema,[4] Jacob van den Born,[1] Stefan P. Berger[1]; the COMBAT Consortium

[1]*Division of Nephrology, University Medical Center Groningen, University of Groningen, Groningen, The Netherlands;* [2]*Department of Surgery, University Medical Center Groningen, University of Groningen, Groningen, The Netherlands;* [3]*Transplantation Immunology, Department of Laboratory Medicine, University of Groningen, University Medical Center Groningen, Groningen, The Netherlands; and* [4]*Medical Biology Section, Department of Pathology and Medical Biology, University Medical Center Groningen, University of Groningen, The Netherlands*

Abstract

Renal endothelial cells (ECs) play crucial roles in vasorelaxation, ultrafiltration, and selective transport of electrolytes and water, but also in leakage of the glomerular filtration barrier and inflammatory processes like complement activation and leukocyte recruitment. In addition, they are target cells for both cellular and antibody-mediated rejection in the transplanted kidney. To study the molecular and cellular processes underlying EC behavior in renal disease, well-characterized primary renal ECs are indispensible. In this report, we describe a straightforward procedure to isolate ECs from the perfusion fluid of human donor kidneys by a combination of negative selection of monocytes/macrophages, positive selection by CD31 Dynabeads, and propagation in endothelium-specific culture medium. Thus, we isolated and propagated renal ECs from 102 donor kidneys, representative of all blood groups and major human leukocyte antigen (HLA) class I and II antigens. The obtained ECs were positive for CD31 and von Willebrand factor, expressed other endothelial markers such as CD34, VEGF receptor-2, TIE2, and plasmalemmal vesicle associated protein-1 to a variable extent, and were negative for the monocyte marker CD14 and lymphatic endothelial marker podoplanin. HLA class II was either constitutively expressed or could be induced by interferon-γ. Furthermore, as a proof of principle, we showed the diagnostic value of this renal endothelial biobank in renal endothelium-specific cross-matching tests for HLA antibodies.

NEW & NOTEWORTHY We describe a new and widely accessible approach to obtain human primary renal endothelial cells in a standardized fashion, by isolating from the perfusate of machine-perfused donor kidneys. Characterization of the cells showed a mixed population originating from different compartments of the kidney. As a proof of principle, we demonstrated a possible diagnostic application in an endothelium-specific cross-match. Next to transplantation, we foresee further applications in the field renal endothelial research.

donation; endothelial cells; kidney; machine perfusion; perfusate; transplantation

INTRODUCTION

The endothelium covers the inner surface of all blood vessels in our body and therefore resides at the critical interface between blood and tissue. The endothelium plays an important role in innate and adaptive immunity and is involved in various disease states, either as a primary determinant of pathophysiology or as a responder to secondary stage damage (1–3). No two endothelial cells (ECs) are alike, although a few universal phenotype markers are known, including CD31 and CD34. The endothelium has different functions, corresponding to the region of the body where it is situated (3). A number of studies have shown molecular heterogeneity at the level of the endothelium, e.g., serial analysis of gene expression has uncovered several transcripts that are selectively expressed in glomerular ECs but not on aortic ECs (4). Also within the kidney, heterogeneity in the endothelium is impressive, as shown by single-cell mRNA profiling (5, 6).

An important corollary of endothelial heterogeneity in the kidney is the unique response of each vascular segment to pathophysiological processes (5, 7). In kidney transplantation, the first immunological barrier that the recipient's immune system encounters is the donor's endothelium, turning ECs into the primary target of the alloimmune response (8). ECs

within the renal vasculature thus become the target of circulating antibodies against human leukocyte antigens (HLAs) and anti-EC antibodies (AECAs), resulting in antibody-mediated rejection (ABMR) (9). ABMR is a leading cause of graft dysfunction and inferior outcomes after transplantation and is often unresponsive to current therapies (10). Vascular inflammation, injury, and complement deposition along the microvascular branches are diagnostic criteria in ABMR, but the pathophysiology of the vascular damage is not fully understood (11, 12). Consequently, ABMR remains a diagnostic and therapeutic challenge.

Multiple groups have tried to address the role of endothelial responses to HLA and non-HLA antibodies; however, several hurdles hamper the clarification of endothelium-antibody interplay. EC research is commonly based on widely available primary EC cultures like human umbilical vein ECs (HUVECs): macrovascular venous endothelium derived from immune-privileged fetal tissue, which is not representative of the adult endothelium (13, 14). In addition, EC cross-matches and renal-related EC assays with cells like human arterial ECs and human dermal microvascular ECs do not take the physiological and phenotypic heterogeneity of the endothelium into account and may underestimate the distinction of the renal microvascular endothelium (15–18). To our knowledge, only one renal glomerular EC line (CiGeNC) (19) is widely used, and Delville et al. recently developed a non-anti-HLA AECA cross-match assay using CiGeNC. They confirmed specific renal microvascular EC responses and revealed substantial differences in activation profiles between macrovascular and microvascular ECs in response to AECAs (9). However, from cross-matching comparison studies, it appeared that it is both the nature of the heterogenous mixtures of antibodies and the particular set of antigens on the target cells that determine the effectiveness of antibody-antigen binding and complement activation (20). Since CiGeNC are derived from only one donor with a specific blood group and HLA and endothelial antigen expression profile, the clinical relevance of cross-matching potential recipients with this cell line is limited. Therefore, we investigated whether kidney machine perfusate after organ donation could serve as a source for renal-specific ECs, thereby creating the possibility to isolate ECs from multiple human donors with different blood groups and HLA profiles.

MATERIALS AND METHODS

Isolation of Machine Perfusion-Derived Primary Renal ECs

Experiments were performed with cells derived from machine perfusates after deceased donor kidney donation. The study was approved by the Institutional Review Board of University Medical Center Groningen (UMCG), adheres to the Declaration of Helsinki and Istanbul, and has NCT0327841 as its ClinicalTrial.gov identifier. Hypothermic machine perfusion is currently the standard storage method for deceased donor kidneys in The Netherlands, using either LifePort 1.1 (Organ Recovery Systems, Zaventem, Belgium) or the Kidney Assist (KA) transporter (Organ Assist, Groningen, The Netherlands). Both machines are pressure controlled (set at a mean of 25 mmHg) (21) and use University of Wisconsin machine perfusion solution (22). After removal of the kidney from the machine, the remaining perfusion fluid was resuspended. For the LifePort disposable, the filter was retrogradely flushed to retrieve cells caught in the filter. Perfusion fluid was collected in sterile 500-mL containers (Cat. No. CLS431123, Corning Sigma) and centrifuged at 4°C for 15 min at 300 g. After removal of the supernatant, cells were washed with culture medium [medium 200 (M200), Cat. No. M-200-500, Gibco, Grand Island, NY] containing Low Serum Growth Supplement (Cat. No. S-003-K, Gibco). After a second washing step with culture medium, plastic-based negative selection was performed to remove monocytes, by incubating the cells for 1 h at 37°C in an uncoated T75 culture flask (23).

After 1 h, nonadherent cells were distributed in a single well of a six-well culture plate (10 cm^2) precoated with 1% gelatin (Cat. No. G1890-100G, Sigma-Aldrich, Darmstadt, Germany). Cells were incubated at 37°C, and culture medium was changed every 2 days.

CD31 immunomagnetic beads (Dynabeads CD31, Ref. No. 11155D, Invitrogen, Landsmeer, The Netherlands) were used for positive selection of renal ECs from the mixture of cultured cells. After ~2 wk of culturing, the number of ECs was estimated by eye, based on confluence and morphology of the cells in culture. Next, the amount of CD31 Dynabeads solution was estimated aiming at 4 beads/cell. Beads were washed and diluted in bead wash buffer (Cat. No. A1595, Sigma-Aldrich) with 0.1% BSA (Cat. No. A9647-100G, Sigma-Aldrich) supplemented with gentamycine (BE02-012E, Lonza, Basel, Switzerland). Cells were detached using trypsin-EDTA (Cat. No. 59430C, Sigma-Aldrich), which was subsequently neutralized using trypsin neutralizer solution (Cat. No. R-002-100, Gibco). Cells were centrifuged (4°C, 1,500 RPM, 7 min), the supernatant was removed, and cells were incubated with CD31 Dynabeads in 200-μL bead wash at 20°C for 20 min on a roller bank. Thereafter, the cell-CD31 Dynabeads mixture was placed in a magnet for 2 min, followed by removal of the supernatant and two additional washing steps of the beaded cells with bead wash buffer. Once the machine perfusion-derived primary renal ECs (MP-PRECs) had been purified, they were cultured in M200 with low-serum growth supplement. To visualize all cells present in the primary perfusate, cytospins were made directly after isolation and before plastic-based negative selection, containing 1,000,000 cells/mL. Differentiation of white blood cell populations in the primary perfusate was analyzed using a Sysmex XN series analyzer (Sysmex, Kobe, Japan) and by May–Grunwald–Giemsa (MGG) staining. Detailed protocols of the isolation techniques are provided in the APPENDIX A and APPENDIX B.

Flow Cytometry

Cells were stained by flow cytometry directly after isolation; nonadherent and adherent cells were stained after plastic-based negative selection, and MP-PRECs were stained at 7 and 21 days after positive CD31 Dynabeads selection. Before the staining procedure, excess erythrocytes in the perfusion fluid from the donor were lysed using lysis buffer (155 mmol/L NH$_4$Cl, 10 mmol/L KHCO$_3$, and 0.1 mmol/L EDTA, Pharmacy UMCG, Groningen, The Netherlands). Details on antibodies and conjugates used for flow cytometry are shown in Table 1.

Table 1. *Details on the primary antibodies and conjugates used in flow cytometry and (confocal) immunofluorescence staining procedures*

Technique	Marker	Antibody	Conjugate
Flow cytometry	CD31	PE-conjugated mouse anti-human CD31 (ready to use, IQP-552R, IQ Products, Groningen, The Netherlands)	
Flow cytometry	CD45	PerCP-Cy 5.5-conjugated mouse anti-human CD45 (clone HI30, BD Biosciences, San Jose, CA)	
Flow cytometry	CD14	Alexa Fluor 700-conjugated mouse anti-human CD14 (clone M5E2, Cat. No. 557923, BD Biosciences)	
Flow cytometry	Tie2/TEK	Mouse anti-human Tie2/TEK [1:25, clone 33.1 (Ab33), Biolegend, San Diego, CA]	Goat anti-mouse FITC (Cat. No. 1031-02, Southern BioTech)
Flow cytometry	HLA class I	Mouse anti-human HLA A-B-C (1:100, clone W6/32, Bio-Rad, Kidlington, UK)	Goat anti-mouse IgG FITC (1:100, Cat. No. 1031-02, Southern BioTech)
Flow cytometry	L-selectin	Mouse anti-human CD62L (1:100, Cat. No. 555542, BD Pharmingen, San Jose, CA)	Goat anti-mouse IgG FITC (1:100, Cat. No. 1031-02, Southern BioTech)
Flow cytometry Immunofluorescence	HLA class II	APC-conjugated mouse anti-human HLA-DR (1:50, clone L243, Cat. No. 347403, BD Biosciences)	
	Isotype control		PE-conjugated rabbit anti-mouse IgG1 (1:10 dilution of IW Products F(ab)^2 IQ Products, IQP-190R)
Immunofluorescence	Von Willebrand factor	Sheep anti-human von Willebrand factor (1:1,000, AHP062, Bio-Rad)	Donkey anti-sheep Alexa 488 (A11015, Invitrogen)
Immunofluorescence	Podoplanin	Mouse anti-human podoplanin (1:100, clone D2-40, Ref. No. M3619, DAKO)	Donkey anti-mouse Alexa 647 (1:250, P0447, DAKO)
Immunofluorescence	VEGFR-2	Rabbit anti-human VEGFR-2 (1:200, clone D5B1, No. 9698, Cell Signaling Technology)	Goat anti-rabbit IgG-horseradish peroxidase + tetramethylrhodamine tyramide reagent (tyramide-TRITC) (1:50, FPI051, Perkin-Elmer LAS, Boston, MA)
Immunofluorescence	PV-1	Mouse anti-human PV-1 (1:50, MON60001-1)	Donkey anti-mouse Alexa 647 (1:250, P0447, DAKO)
Immunofluorescence	Activated C3	Mouse anti-human activated C3 (HM2168, Hycult, Uden, The Netherlands)	Goat anti-mouse IgG FITC (Cat. No. 1031-02, Southern BioTech)

HLA, human leukocyte antigen; PV-1, plasmalemmal vesicle-associated protein-1; Tie2/TEK, tyrosine kinase transmembrane receptor; VEGFR-2, vascular endothelial growth factor receptor-2.

All antibodies were diluted in 1% BSA in PBS and then incubated for 30 min on ice. Isotype and conjugate controls were included for all stainings. HUVECs obtained from the UMCG endothelial facility were used as a control for CD31 expression (24). Cell culture contamination with peripheral blood mononuclear cells (PBMCs) was examined with PBMC markers CD14 and L-selectin (23, 25). For the measurement of HLA class I and II expression, cells were stimulated for 48 h with 50 ng/mL interferon (IFN)-γ in M200 at 37°C. The percentage of IFN-γ-induced HLA expression was calculated as the increase in % = 100 − [mean fluorescence intensity (MFI) unstimulated cells × 100)/MFI stimulated cells]. Cells were analyzed using a FACSCalibur equipped with CELLQuest software and Kaluza software (Kaluza 2.1 Becker Coulter).

Immunofluorescence

Endothelial phenotyping was performed on MP-PRECs from different donors (*n* = 8). Cells were grown on Lab-Tek chamber slides (Ref. No. 177445, Thermo Fisher Scientific, Groningen, The Netherlands) coated with 1% gelatin for 30 min. Cells were fixed with 4% paraformaldehyde in PBS for 10 min at room temperature, incubated with 0.5% Triton X-100 in PBS for 10 min, and then blocked with 2% BSA for 30 min. All primary and secondary antibodies were diluted with 1% BSA in PBS and then incubated for 1 h at room temperature. Details on antibodies and conjugates used for immunofluorescence are shown in Table 1. All sections were counterstained for 10 min with DAPI (0.001 mg/mL in PBS, Ref. No. D954, Sigma). Pictures were taken and evaluated on a Leica DM4000B equipped for immunofluorescence and with a TissueFaxs using Tissue Quest (Tissuegnostics, Medical & Biotech Solutions, Vienna, Austria) as digital quantification software.

Quantitative RT-PCR

For the characterization of endothelium-specific gene expression, quantitative RT-PCR was performed. RNA was isolated from MP-PRECs on *days 0* and *7* after CD31 Dynabeads selection using the RNease Micro Plus Kit (Qiagen, Venlo, The Netherlands) according to the manufacturer's instructions. cDNA was synthesized using Superscript III Reverse Transcriptase (Invitrogen). Taqman assays (Applied Biosystems, Nieuwekerk aan den IJssel, The Netherlands) were used to perform gene expression analysis. Human-specific

primers were selected to amplify CD31, CD34, von Willebrand factor (vWF), plasmalemmal vesicle-associated protein-1 (PV-1), vascular endothelial growth receptor-2 (VEGFR-2), HLA-DR, angiotensin II receptor type 1, α_2-smooth muscle actin (ACTA2; α_2-SMA), platelet-derived growth factor-B (PDGF-B) for (myo) fibroblasts, and/or mesangial cells and nephrin (NPHS1) for podocytes (Table 2). Glyceraldehyde-3-phosphate dehydrogenase (GAPDH) was used as a housekeeping gene. PCR amplification was performed in a ViiA 7 real-time PCR System (Applied Biosystems) according to the manufacturer's protocol. Duplicate real-time PCRs were performed for each sample, and the obtained threshold cycle (C_T) values were averaged. Gene expression reactions were normalized to the averaged expression of the housekeeping gene, yielding the ΔC_T value. Relative gene expression levels were calculated by $2^{-\Delta CT}$.

Proof of Principle: Complement Activation Using MP-PRECs

The complement-activating capacity of MP-PRECs was evaluated by classical complement activation. In a custom EC cross-match assay, cells were incubated with human monoclonal anti-HLA antibodies (A2/A28 IgG1 and Bw6 IgG1, a kind gift from Dr. F. Claas, Leiden, The Netherlands), 25% heat-inactivated (HI) (1 h at 56°C) human serum containing HLA antibodies directed against HLA antigens expressed on the MP-PREC cell membrane, and 25% HI blood group-incompatible serum diluted in M200 for 45 min. A 25% HI blood group compatible serum and HI serum containing HLA antibodies not directed against HLA antigens expressed on the MP-PREC cell membrane were used as controls. After two washes with M200, 20% pooled AB serum from healthy volunteers was used as a complement source, and cells were incubated for 30 min before two washes with 1% BSA. Complement activation was measured using anti-human activated C3 (recognizing the cleavage fragments of C3b, iC3b, and C3c) (Table 1). Immunofluorescent pictures were taken and analyzed as described above in *Immunofluorescence*.

RESULTS

Isolation of MP-PRECs

From January 2017 until July 2019, 102 donor kidney perfusates were isolated after deceased kidney donation

Table 2. *Primers*

Species	Gene	Human Assay ID
Homo sapiens	GAPDH	Hs99999905_m1
Homo sapiens	PECAM-1 (CD31)	Hs00169777_m1
Homo sapiens	CD34	Hs00990732_m1
Homo sapiens	Von Willebrand factor	Hs00169795_m1
Homo sapiens	PV-1 (PLVAP/MECA32)	Hs00229941_m1
Homo sapiens	VEGFR-2 (KDR)	Hs00176676_m1
Homo sapiens	HLA-DR	Hs99999917_m1
Homo sapiens	AGTR1	Hs00258938_m1
Homo sapiens	α_2-SMA (ACTA2)	Hs00909449_m1
Homo sapiens	NPHS1	Hs00190446_m1
Homo sapiens	PDGF-B	Hs00234042_m1

α_2-SMA, α_2-smooth muscle actin; AGTR1, angiotensin II receptor type 1; HLA, human leukocyte antigen; NPHS1, nephrin; PDGF-B, platelet-derived growth factor-B; PECAM-1, platelet endothelial cell adhesion molecule-1; PV-1, plasmalemmal vesicle-associated protein-1; VEGFR-2, vascular endothelial growth factor receptor-2.

according to the procedure shown in Fig. 1. Of the 102 EC isolations, 41% were from the KA perfusion device and 59% from the LifePort (Table 3). MP-PRECs equipped with a large variety of HLA types (Table 4) and blood groups (Table 5) were obtained, which were representative of the general population compared with the percentage of antigens within a pool of 10,000 recent organ donors (26). Further clinical characteristics are shown in Table 3. After successful CD31 Dynabeads selection, 27% of cultures became infected and 25% stopped proliferating between *days 7* and *21*. The success rate (defined as 1×10^6 MP-PREC yield to perform an experiment with/store in liquid nitrogen) was 39% (40 isolates).

For all isolations, the time between the isolation of cells from the perfusate and CD31 Dynabeads selection (*passage 0* to *passage 1*) was 18.1 ± 3.5 days. The first passage thereafter (*passage 1* to *passage 2*) was 8.3 ± 3.4 days after reseeding, at an average of 60,000 cells per cm^2 (Supplemental Table S1; see https://doi.org/10.6084/m9.figshare.13103003). MP-PRECs were stored in liquid nitrogen or used for phenotyping and/or antibody-mediated complement activation experiments between *passages 3* and *7*.

MGG and Flow Cytometry of Perfusate Cells

Five-pas leukocyte differentiation and MGG staining on cytospins ($n = 2$ replicates) of perfusate cells showed a mixture of leukocytes, of which ∼30% were polynuclear cells (neutrophils) and ∼70% were mononuclear cells (Fig. 2 and Supplemental Table S2; see https://doi.org/10.6084/m9.figshare.13676902). FACS scatterplots revealed three clearly identifiable cellular groups, presumably representing neutrophils, lymphocytes, and monocytes, next to ECs. Within the monocytic cellular group, a minority of the cells were CD31$^+$, CD14$^-$, and CD45$^-$. These likely represent ECs (Supplemental Fig. S1; see https://doi.org/10.6084/m9.figshare.13677019).

Since some leukocytes express CD31 antigens, albeit to a much lower extent compared with ECs (27), they could be contaminating cells in MP-PREC cultures. Flow cytometry showed that 39% of total perfusate cells were CD31$^+$, of which 11% were CD31$^+$ and CD45$^-$ (Fig. 2, *B–D*). This indicates that ±4% of cells in the perfusate are in fact ECs.

Effective Removal of CD31 CD14 Double-Positive Cells From Perfusate Cells by Plastic Adherence

Since MGG staining of perfusate cells showed possible MP-PREC culture contamination by CD31$^+$ leukocytes, we performed a negative selection technique to remove contaminating cells from the same hematopoietic lineage as ECs, in particular monocytes. As monocytes adhere to plastic within 30 min of incubation whereas ECs do not, plastic-based negative selection was used (23). Cells from the perfusate, before and after negative selection, were evaluated by flow cytometry. 20% of the cells before selection expressed high levels of CD31 and CD14 (Fig. 3), identifying them as monocytes, and 39% of the cells expressed only CD31 (Fig. 3). With plastic-based negative selection, CD14$^+$CD31$^+$ cells adhered to the plastic (Fig. 3) and CD14$^-$CD31$^+$ cells remained nonadherent (Fig. 3). Therefore, the selection resulted in the depletion of CD14$^+$CD31$^+$ cells from the original cell suspension. A subset of the cells expressed neither CD14 nor CD31. These
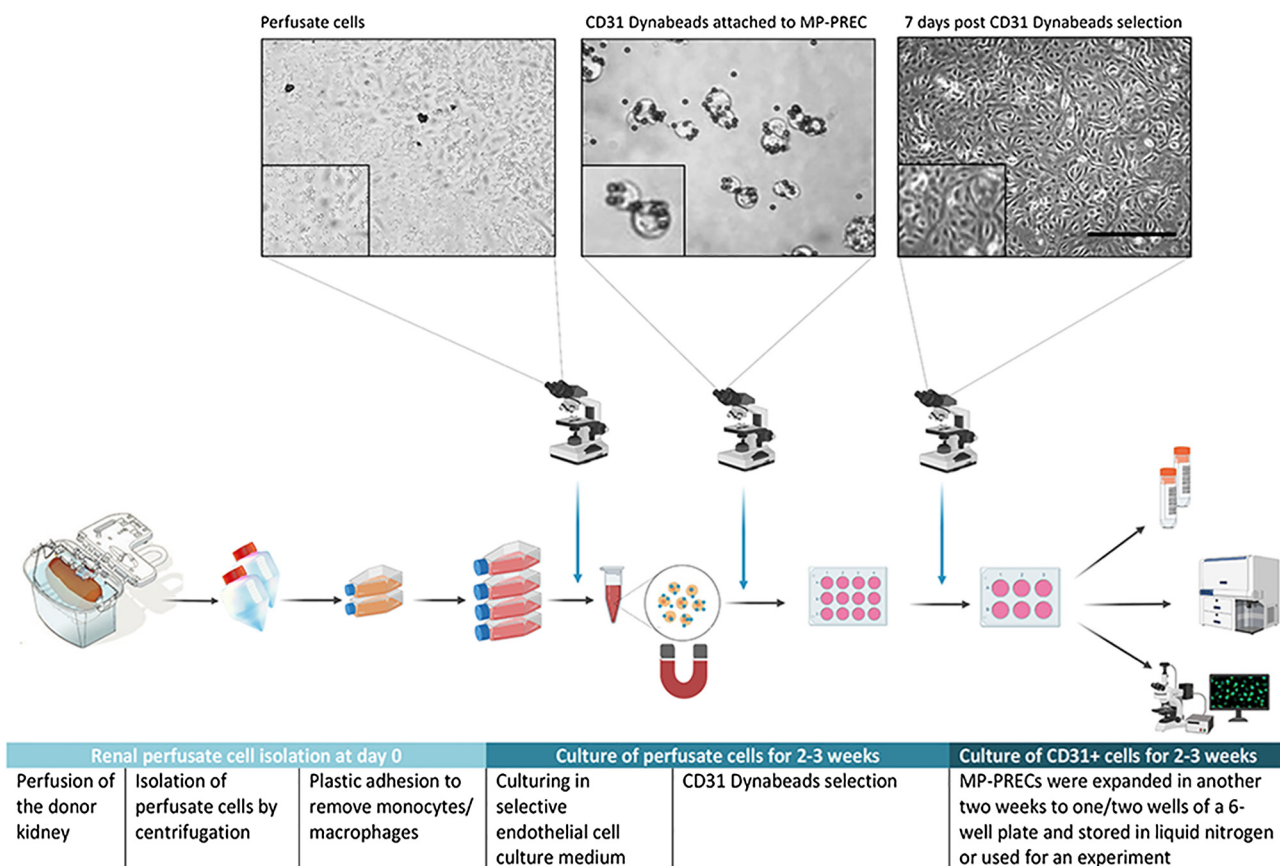
Figure 1. Isolation procedure of machine perfusion-derived primary renal endothelial cells (MP-PRECs). Scale bar = 200 μm. [Figure created with Biorender.com.]

CD14⁻CD31⁻ cells were smaller in size in the forward scatter and showed a low granularity in the sideward scatter and likely represent lymphocytes that will be removed from the cell culture after CD31 Dynabeads selection.

MP-PRECs Regain Morphological EC Appearances and Retain CD31 Expression After Prolonged Time in Culture

CD31 is a pan EC marker expressed on the EC membrane and is suitable for the isolation of MP-PRECs using CD31 Dynabeads selection. This procedure did not affect the growth of MP-PRECs, since MP-PRECs could be cultured after the CD31 Dynabeads procedure with the beads still attached (Fig. 4A). After ~7 days and two to three medium replacement steps, the beads had fully detached from the cell membrane and MP-PRECs showed features of primary culture ECs with the formation of "cobblestone" monolayers (Fig. 4B). At 7 and 21 days after CD31 Dynabeads selection and culture, a distinct peak of MP-PRECs with CD31 cell surface expression was found, comparable with that of HUVECs (Fig. 4). Seven days after CD31 Dynabeads selection and culture, the mean CD31 MFI was 98.2 ± 14.9 compared with the mean CD31 MFI of 88.3 ± 22.6 at 21 days after CD31 Dynabeads and culture (P = 0.49; Fig. 4).

CD31 is expressed on the cell membrane of all ECs and rarely on any other cell type (27). However, overgrowth for contaminating cell types was investigated by flow cytometry analysis of cultured MP-PRECs for CD31 cell surface expression and for the PBMC surface expression markers CD14 and L-selectin. At 28 days after CD31 Dynabeads selection, no CD14 and L-selectin cell surface expression was found (Supplemental Fig. S2; see https://doi.org/10.6084/m9.figshare.13677067).

EC Markers Expressed by MP-PRECs Show Variation Between Donors

Since flow cytometry showed that MP-PRECs express CD31 on the cell membrane, different EC markers were selected as glomerular, peritubular, microvascular, and macrovascular EC markers for further endothelial phenotyping. CD31, CD34, and Tie2/TEK were selected as general endothelium-restricted markers (28, 29), vWF was selected as a macrovascular marker (30, 31), VEGFR-2 was selected as a glomerular and peritubular microvascular marker (32), PV-1 was selected as a purely peritubular microvascular marker (33), and podoplanin was selected as a lymphatic endothelial marker (34).

Using quantitative RT-PCR, expression of the EC markers CD31, CD34, vWF, PV-1, VEGFR-2, and HLA-DR were assessed on two different MP-PREC isolates: directly after CD31 Dynabeads selection (*day 0*) and after 7 days of culturing. CD31 mRNA expression levels remained stable throughout culture in both isolates and vWF increased over time, whereas CD34, PV-1, and VEGFR-2 remained relatively low or were lost over time. HLA-DR remained either present or not expressed (Fig. 5A). No AGTR1 mRNA expression was

Table 3. *Baseline characteristics of postmortem organ donors at the time of death*

Variable	Value
Age, yr	59 ± 17
Male sex (*n*, %)	56 (54.9)
Height, cm	175 ± 14
Weight, kg	80 ± 20
Body mass index, kg/cm^2	25.50 ± 5
Mean arterial pressure, mmHg	91 ± 21
Donor type DBD (*n*, %)	31 (30.4)
Hypotension at ICU (*n*, %)	23 (22.5)
Time hypotension at ICU, min	0 ± 0
Hypertension in medical history (*n*, %)	28 (27.5)
Cause of death	
Circulational	20 (19.6)
Respirational	2 (2.0)
Trauma	14 (13.7)
Cerebrovascular accident	29 (28.5)
Subarachnoidal bleeding	18 (17.6)
Subdural hematoma	2 (2.0)
Suicide	8 (7.8)
Euthanasia	2 (2.0)
Medical complication	1 (1.0)
Meningitis	1 (1.0)
Not specified	5 (4.9)
Smoking at time of death (*n*, %)	48 (47.1)
Diabetes mellitus (*n*, %)	4 (3.9)
Kidney preservation (Kidney Assist/Lifeport)	42/60

Normally distributed data are presented as means ± SD, skewed data are presented as medians (interquartile ranges), and categorical data are presented as number (percentage) (*n*, %). DBD, donor after brain death; ICU, intensive care unit.

found (data not shown). Using quantitative RT-PCR, four MP-PREC isolates were tested for contamination with mesangial cells, (myo)fibroblasts, and podocytes. All four cell cultures were negative for nephrin at *day 0*, *day 1*, and *day 7* after CD31 Dynabeads selection, excluding contamination with podocytes. Three of four cell cultures were negative for ACTA2 and PDGF-B mRNA expression 7 days after CD31 Dynabeads isolation, excluding contamination with mesangial cells and/or (myo)fibroblasts in the MP-PREC cell culture. However, in one cell culture, transcripts for both ACTA and PDGF-B could be found (Supplemental Fig. S3; see https://doi.org/10.6084/m9.figshare.13677220).

Immunofluorescence staining showed heterogeneous expression of vWF, VEGFR-2, and PV-1 on MP-PRECs from different donors after CD31 Dynabeads selection and culture for at least 21 days. Variation was observed in the number of positive cells and the intensity of staining. Discrete intracellular structures resembling Weibel–Palade bodies were found, albeit vWF was expressed to various extents between donors. MP-PRECs from some donors expressed VEGFR-2, whereas in cells from another donor, VEGFR-2 expression was sparse. Some MP-PRECs isolates also expressed PV-1 and HLA-II, albeit to varying extents (Fig. 5B). None of the MP-PREC isolates expressed the lymphatic EC marker podoplanin (*n* = 4 replicates; Supplemental Fig. S4; see https://doi.org/10.6084/m9.figshare.13677253).

Double staining for vWF and VEGFR-2 also revealed variability between MP-PREC cultures (*n* = 3 replicates; see Supplemental Fig. S5; see https://doi.org/10.6084/m9.figshare.13677298).

Flow cytometry using MP-PRECs from three different donors at 7, 9, and 21 days after CD31 Dynabeads selection

Table 4. *Frequency of the most common human leukocyte antigen alleles in the MP-PREC databank compared with the frequency in the Eurotransplant databank* (https://www.etrl.org/)

Allele	Eurotransplant, % (*n* = 10,000)	Biobank, % (*n* = 102)
A1	27	26
A2	51	51
A3	27	31
A9	22	22
A19	24	18
A24	18	18
B7	23	26
B12	23	22
B35	19	17
B44	23	22
Bw4	61	48
Bw6	85	89
Cw3	25	38
Cw4	23	23
Cw6	18	15
Cw7	50	59
Cw9	25	18
Cw10	25	18
DR2	30	27
DR5	28	17
DR6	30	31
DR51	30	27
DR52	67	68
DR53	40	37
DQ1	68	78
DQ2	35	35
DQ3	57	61
DQ5	35	34
DQ6	42	43
DQ7	37	30

MP-PREC, machine perfusion-derived primary renal endothelial cell.

showed that CD31 was continuously expressed, along with varying (donor-dependent) expression of Tie-2/TEK, VEGFR-2, and vWF. HUVECs were used as a control (Fig. 5C). Variation in the expression of EC markers was a consistent observation in all donors examined.

HLA Loci on MP-PRECs

Since we developed the MP-PREC isolation technique for the purpose of detection of antibodies directed against antigens expressed by ECs, HLA antigen expression of MP-PRECs was analyzed under IFN-γ-stimulated conditions. Expression of pan HLA-I and the HLA-II-DR locus by MP-PRECs increased by 50% and 30%, respectively, when stimulated with IFN-γ, as assessed by flow cytometry (*n* = 2 replicates; Fig. 6A).

Table 5. *Frequency of blood groups A, B, O, and AB in the MP-PREC databank compared with the frequency in the Eurotransplant databank* (https://www.etrl.org/)

Blood Group	Eurotransplant, % (*n* = 10,000)	Biobank, % (*n* = 102)
A	43	46
B	12	5
O	40	45
AB	5	4

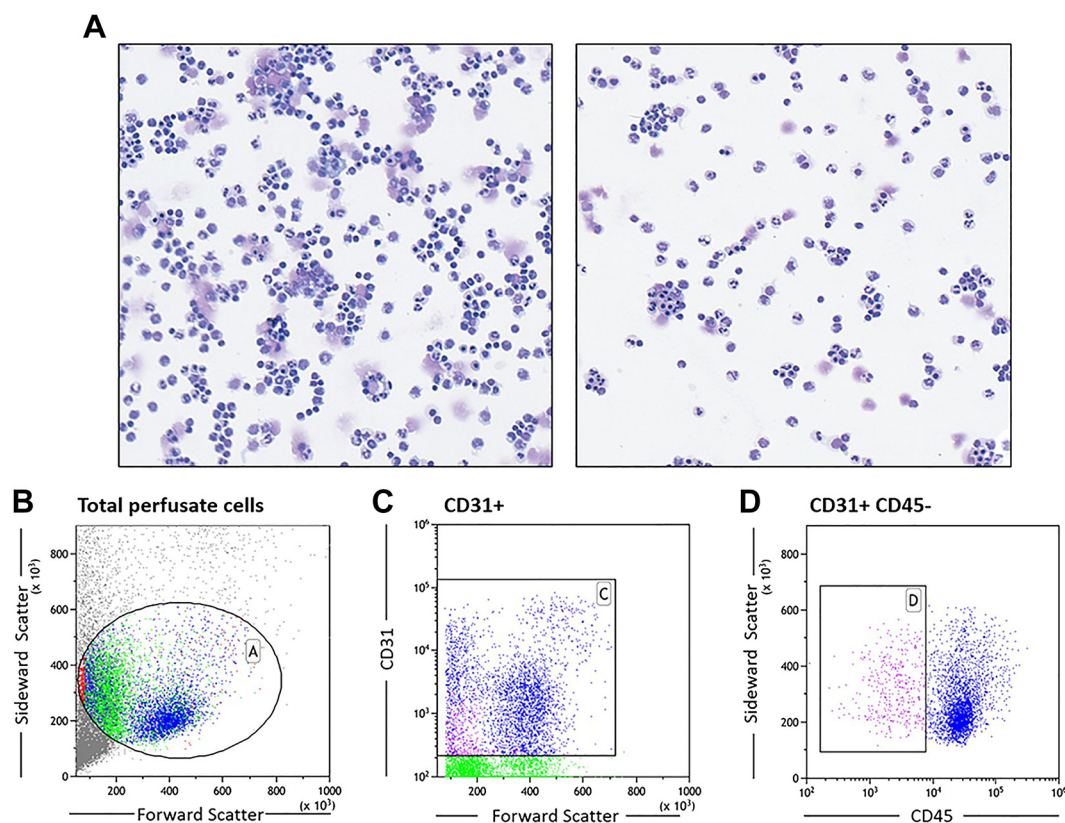MP-PREC, machine perfusion-derived primary renal endothelial cell.

Figure 2. May–Grunwald–Giemsa staining and flow cytometry double staining on perfusate cells. *A*: representative images of May–Grunwald–Giemsa staining on cytospins of perfusate cells from two different donors showing monocytes, lymphocytes, and neutrophils. *B*: flow cytometry showing the total amount of cells in the perfusate fluid after kidney perfusion. *C* and *D*: 39% of the perfusate cells were CD31$^+$ (*C*), of which 11% were CD31$^+$ and CD45$^-$ (*D*).

Additional immunofluorescence staining on MP-PRECs of different donors (*n* = 4 replicates) after 21 days in culture revealed variation in induced expression of HLA-DR between unstimulated cells and their corresponding IFN-γ-stimulated cells (Fig. 6, *B* and *C*).

Proof of Principle: Complement Activation on MP-PRECs by Donor-Specific Antibodies

To examine the clinical relevance of MP-PRECs, complement activation, measured as activated C3 deposition on the MP-PREC membrane, was tested with a custom cross-match assay using MP-PRECs from three different donors. Cross-matching with blood group compatible serum consistently showed no complement activation (Fig. 7, *A, F,* and *K*). Cross-matching with blood group incompatible serum (Fig. 7, *B, G,* and *L*), monoclonal HLA antibodies (Fig. 7, *C, H,* and *M*), and sera containing HLA class I and/or class II antibodies directed against HLA antigens expressed on the MP-PREC membrane (Fig. 7, *D* and *I*) resulted in complement C3 activation to varying extents. Serum containing HLA antibodies aspecific for HLA antigens expressed on the MP-PREC membrane did not result in complement activation (Fig. 7N).

DISCUSSION

The lack of availability of primary renal ECs from multiple donors remains a major obstacle when studying the (patho)

physiology of renal ECs and their interindividual variation in reaction to disease processes. Difficulties in obtaining primary cultures of renal EC subsets have hampered molecular characterization, transcriptional profiling, and assay development with ECs. We have developed an EC isolation technique that uses ECs derived from machine perfusates after kidney machine perfusion. We performed isolations after deceased kidney donation, resulting in a bank of primary ECs from multiple donors, featuring general EC characteristics and covering a large spectrum of HLA alleles. These can be used for screening of donor-specific antibodies, but also for other applications.

Although ECs in the human body display many common features, they also reveal remarkable morphological and functional heterogeneity (1, 2). The vasculature of the kidney is not only different from that of other organs but also displays striking intraorgan heterogeneity. Limited accessibility of human kidneys suitable for EC isolations implicates that the majority of research focused on endothelial function in renal diseases is based on the endothelium from diverse origins but generally not the kidney (13, 14, 17, 18, 35–37). The presented method in this study has many advantages over existing supply routes and techniques for EC isolation. First, by taking advantage of the relatively new procedure of organ perfusion between donation and transplantation (38), a continuous supply of donors is guaranteed. Second, the HLA type, blood group, and other characteristics of these cells are
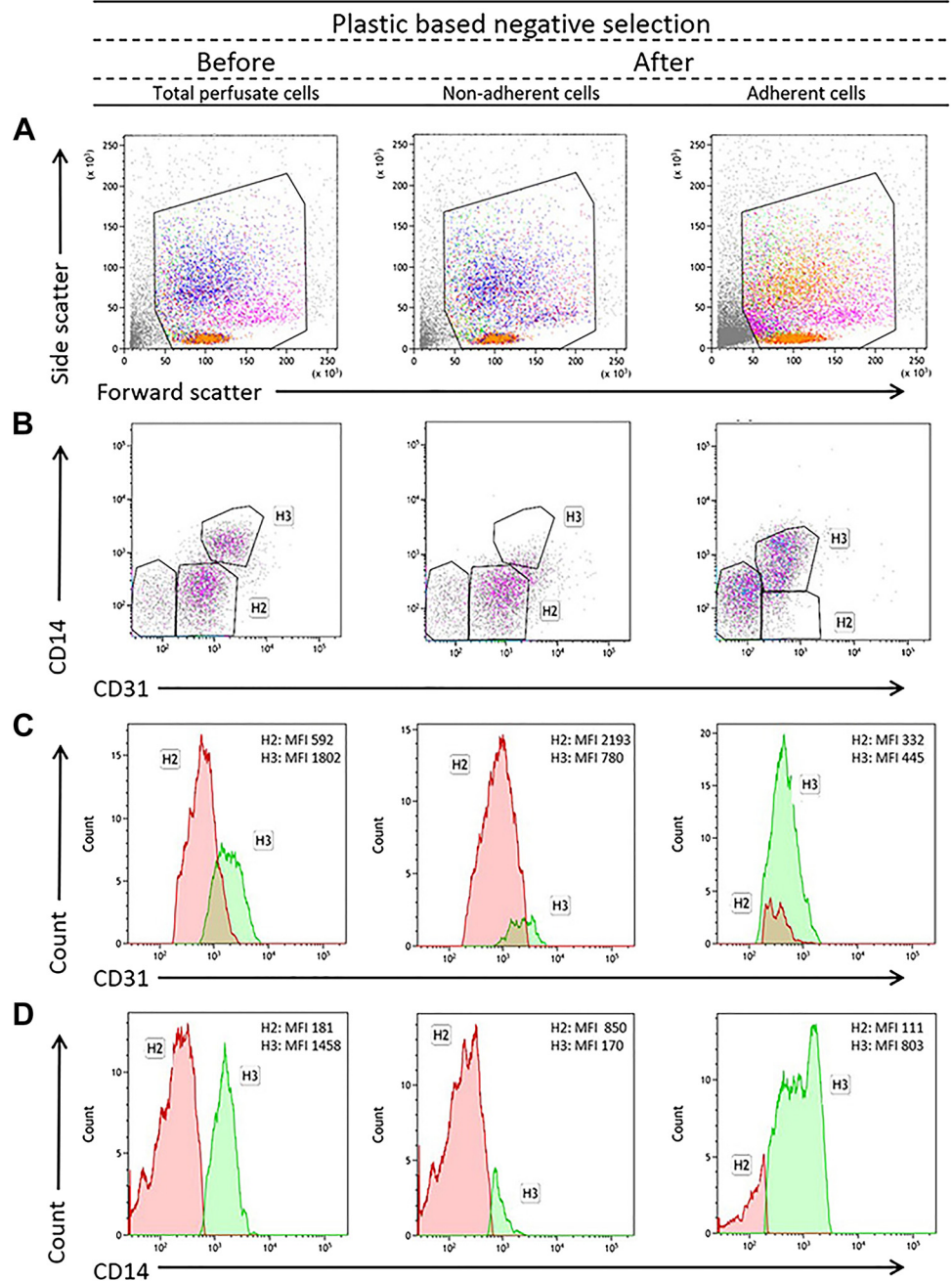
Figure 3. Expression of CD31 and CD14 on perfusate cells and (non)adherent cells after plastic-based negative selection. *A*: flow cytometric analysis showing the forward scatter versus side scatter of cells within total perfusate cells, nonadherent cells, and adherent cells, respectively. *B*: CD31 versus CD14 scatterplots of viable cells within the total perfusate, nonadherent cells, and adherent cells, respectively. Cells in region H2 expressed CD31 alone; cells in region H3 expressed both CD31 and CD14. *C*: single positive CD31 cells in regions H2 and H3 within the total perfusate, nonadherent cells, and adherent cells, respectively. *D*: single positive CD14 cells in regions H2 and H3 within the total perfusate, nonadherent cells, and adherent cells, respectively. Mean fluorescence intensities (MFI) are indicated.

already known. Third, the technique is a relatively easy, nondestructive, and robust method to isolate pure populations of ECs from human donor kidneys. Fourth, apart from the CD31 Dynabeads and culture medium, no special reagents or equipment are needed. This, together with the fact that the perfusate is considered as waste material from the transplantation procedure and no additional procedures are required to harvest human kidneys for EC isolation contributes to the cost effectiveness of this new method. Another major advantage of isolating MP-PRECs is that the cells have an adult tissue origin, as opposed to, for example, HUVECs from a fetal origin. Furthermore, the approach outlined may provide a general strategy for the isolation and culture of ECs from a variety of organs (provided that the organs are perfused). Finally, the method can be used to develop a rich source of renal-specific EC lines for dedicated purposes.

We also acknowledge several disadvantages of the new method. The isolation technique outlined herein is quite time consuming, and as with all cell culture studies, researchers need to be trained. The possible use of FACS was initially investigated for sorting MP-PRECs. Unfortunately, MP-PRECs are vulnerable and relatively large cells, resulting in fragmentation of the cells during the sorting procedure (data not shown). Also, prolonged culture periods and limited yielded cells are important disadvantages of this study. Nevertheless, implementing this isolation method is worth the investment
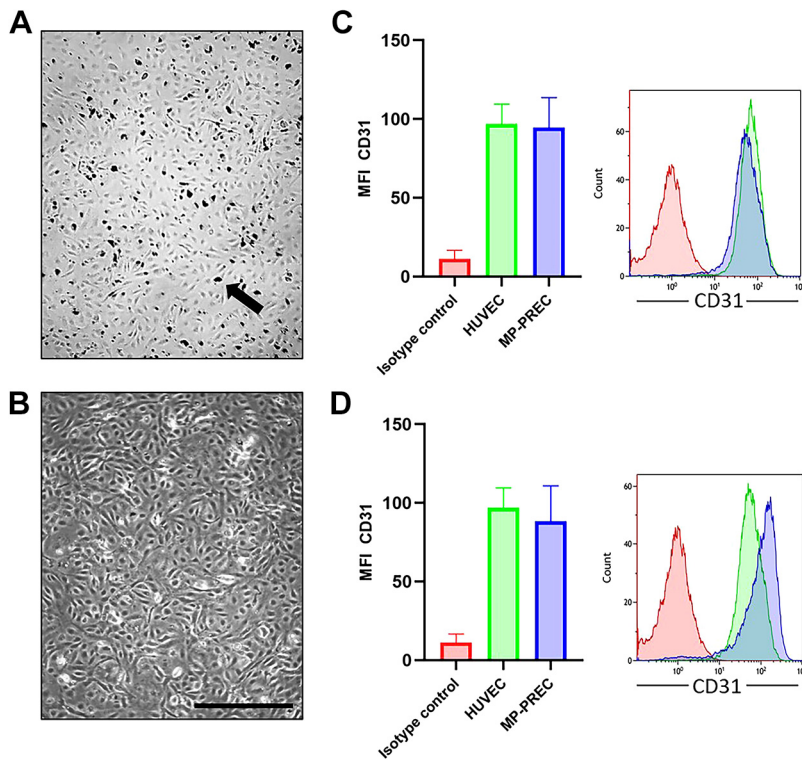
Figure 4. Machine perfusion-derived primary renal endothelial cells (MP-PRECs) maintain endothelial cell appearances. Light microscopy of cultured MP-PRECs at 3 days (*A*) and 7 days (*B*) after CD31 Dynabeads isolation. The arrow points to a cluster of beads. Scale bar = 200 μm. CD31 expression on human umbilical vein endothelial cells (HUVECs) and MP-PRECs was determined by flow cytometry at 7 days (*n* = 4; *C*) and 21 days (*n* = 4; *D*) after culturing. *P* values are indicated. Histograms of a representative experiment show that MP-PRECs (blue) expressed CD31 comparable with HUVECs (green). The isotype control is indicated in red. MFI, mean fluorescence intensity.

as it serves the purpose of isolating ECs from a widely available source of donors, along with the possibilities to develop new applications with MP-PRECs. In addition, as discussed later in this discussion in more detail, the isolated MP-PRECs are heterogeneous in terms of their expression of endothelial cell markers, as shown in Fig. 5, and complement activation, as shown in Fig. 7. This could lessen their utility in studying kidney rejection or other disease processes involving the renal endothelium because every EC isolate would require characterization. Primary ECs are in general a superior model for the in vivo situation since the cell is not manipulated and not affected by multiple passages, when keeping passages low (39). In addition, heterogeneity in response to antibody-mediated complement activation may actually reflect true differences in defense mechanisms to complement-mediated attack between individual donors and thus explain some of the variation of outcome in the presence of donor-specific antibodies. However, the usefulness of primary renal EC culture could be limited by shifts in their in vivo gene expression signature due to the loss of microenvironmental cues (40) and by early onset of senescence (19). Therefore, primary MP-PRECs should be selected based on the gene expression profile in the context of the application of interest and converted into different immortalized cell lines that are then validated thoroughly. The validation process should focus on the expression of endothelium-specific markers during proliferation in cell culture and multiple donor characteristics like antigen expression by repeated gene analyses and protein staining procedures. Before studying a specific research question, one should evaluate the cellular features and gene expression profile based on the application of interest. Thereafter, following common practice in EC biology, EC lines should be continuously

monitored to ascertain their cellular features. Our study is presented as a qualitative methodological paper, as we currently do not have the substantial number of biological replicates of the highly heterogeneous MP-PREC population that would be necessary for a meaningful analysis (41). Therefore, we did not present statistical data on differences in EC expression markers between MP-PREC donors and changes over time. Finally, the risk for contamination with other cells should always be taken into account when working with primary cell cultures. We found some contamination by mesangial and/or renal (myo)fibroblasts in one of four MP-PREC isolates (Supplemental Fig. S3).

The MP-PREC purification strategy was based on the removal of CD31$^+$CD14$^+$ monocytes by plastic adherence, positive selection of CD31$^+$ cells using CD31 Dynabeads, and the use of EC-specific cell culture medium (23). MP-PRECs obtained cobblestone morphological EC appearances when viewed with phase-contrast microscopy, and there was no evidence of overgrowth by contaminating cells (42). MP-PRECs from the majority of donors proliferated in cell culture and therefore appear to be a relatively healthy cell population (43). This raises the following question: why do ECs detach from the renal vasculature during kidney perfusion? It is generally known that ischemia-reperfusion injury after kidney donation substantially contributes to a cascade of harmful events leading to inflammation, endothelial dysfunction, and cell death (44, 45). In vivo, vascular ECs are covered with an endothelial glycocalyx: a gel-like layer consisting of glycoproteins, proteoglycans with bound glycosaminoglycans coating the luminal surface of ECs (46). This layer is vital for EC function as it participates in vascular permeability, microvascular reactivity, and endothelium interaction with blood
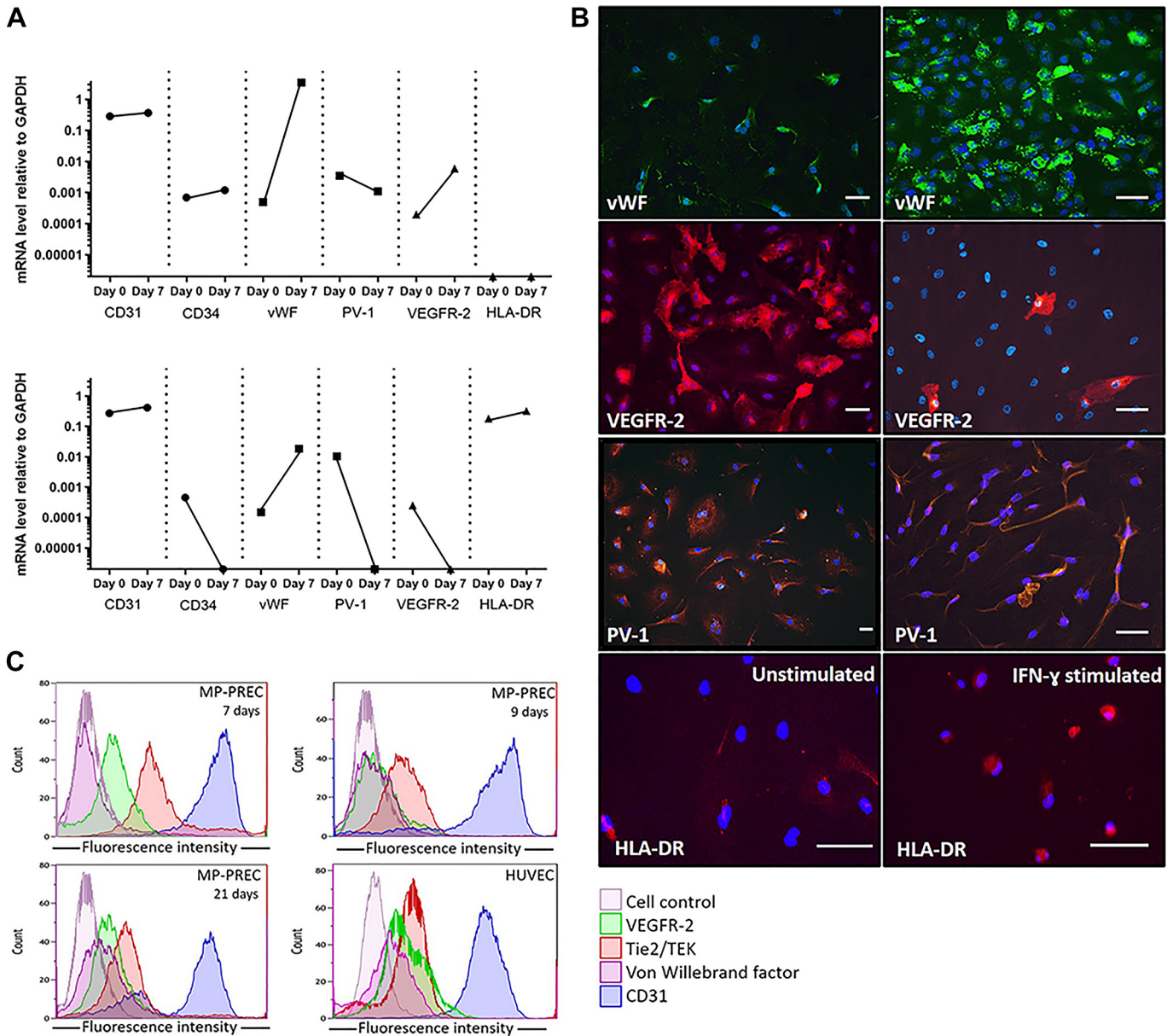
Figure 5. Endothelial cell markers expressed by machine perfusion-derived primary renal endothelial cells (MP-PRECs) show variation among donors. *A*: quantitative RT-PCR showing relative mRNA levels of the following endothelial cell markers: CD31, CD34, von Willebrand factor (vWF), plasmalemmal vesicle-associated protein-1 (PV-1), VEGF receptor (VEGFR)-2, and human leukocyte antigen (HLA)-DR on MP-PRECs from two different donors directly after CD31 Dynabeads selection (*day 0*) and after 7 days of culturing (*day 7*). *B*: immunofluorescence stainings on MP-PRECs from different donors cultured for ~21 days after CD31 Dynabeads selection showing the heterogeneous expression of vWF, VEGFR-2, PV-1, and HLA-DR on unstimulated and interferon (IFN)-γ-stimulated MP-PRECs. Scale bar = 100 μm. *C*: flow cytometry showing expression of VEGFR-2, Tie2/TEK receptor tyrosine kinase (TEK), vWF, and CD31 on MP-PRECs from different donors at 7 days after CD31 Dynabeads selection, 9 days after CD31 Dynabeads selection, and 21 days after CD31 Dynabeads selection compared with human umbilical vein endothelial cells (HUVECs).

constituents. Degradation of the glycocalyx plays an important role in ischemia-reperfusion-related endothelial dysfunction; however, studies on the effect of kidney machine perfusion after the period of ischemia on the renal endothelial glycocalyx are limited (47). Preliminary data show that MP-PRECs produce a glycocalyx, as shown with *Ulex europeus*-1-positive staining of MP-PRECs cultured for ~7 days after CD31 bead selection (data not shown). Further research is needed to assess why the cells detach and whether this is associated with quality and function of MP-PRECs and kidney allograft outcome.

Phenotypic profiling of MP-PRECs from different donors revealed a remarkable variability among isolates and within MP-PRECs originating from one donor, although CD31 remained consistently expressed. Variability was apparent for VEGFR-2, vWF, PV-1, and Tie2/TEK. We showed that MP-PRECs express HLA-I without exception and that HLA-II-DR was either constitutively expressed or could be induced by IFN-γ. The latter is in line with a previous study showing that renal microvascular ECs are able to express HLA class II antigens (48). Our results suggest drift of EC
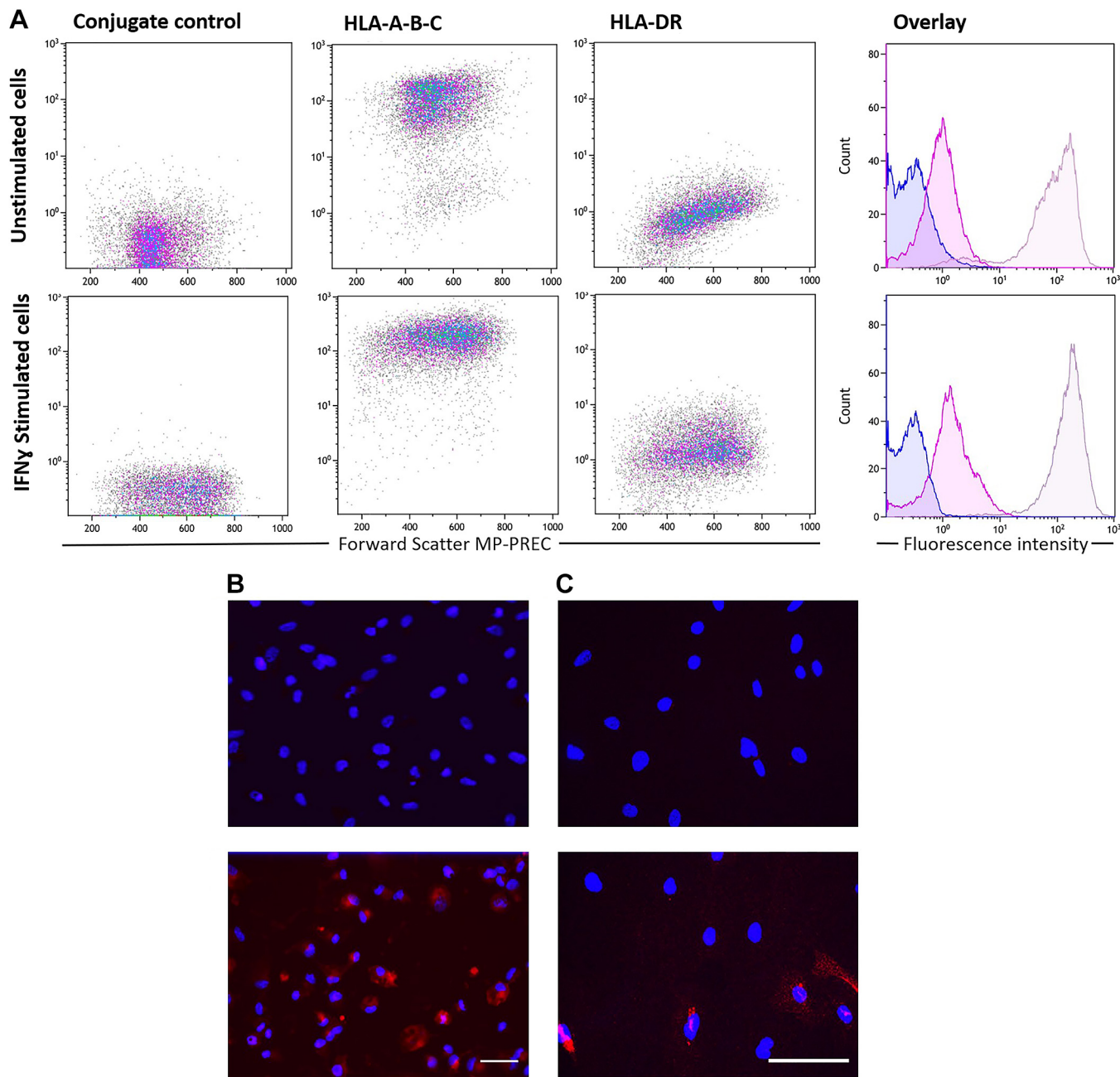
Figure 6. Human leukocyte antigen (HLA) class I and class II expression by machine perfusion-derived primary renal endothelial cells (MP-PRECs). *A*: representative flow cytometry data showing the expression of HLA class I and class II (DR locus) on unstimulated MP-PRECs and interferon (IFN)-γ-stimulated MP-PRECs. Corresponding FACS histograms of unstimulated and stimulated cells are shown in the overlay: HLA class I (pink), HLA class II DR (magenta), and the negative control (blue). *B* and *C*: representative HLA-DR staining on unstimulated MP-PRECs and stimulated MP-PRECs from two different donors. Scale bar = 100 μm.

mRNA expression over time, as exemplified by the loss of microvascular markers PV-1 and VEGFR-2 and increase of vWF in the first week after CD31 Dynabeads isolation. Tie2/TEK was reduced over time in different isolates, as shown with flow cytometry. The reduction of Tie2/TEK could be an indirect effect caused by longer static MP-PREC culture (49). Together, these alterations in culture composition might indicate EC dedifferentiation over time or, alternatively, overgrowth of MP-PRECs from a specific segment (vWF⁺ macrovascular ECs) over time (24, 50). In addition,

MP-PREC immunofluorescent staining for vWF, VEGFR-2, PV-1, and HLA-DR revealed that the distribution of these EC markers within one culture varied for each donor. This likely reflects cultured MP-PRECs obtained from different renal microvasculature structures, having an arterial, glomerular, peritubular, or venous origin (28, 31–33).

One of the aims of this study was to provide a reliable source of renal ECs to investigate the pathogenicity of HLA antibodies on the surface of the primary target of ABMR (9). We therefore focused on developing an EC bank from a
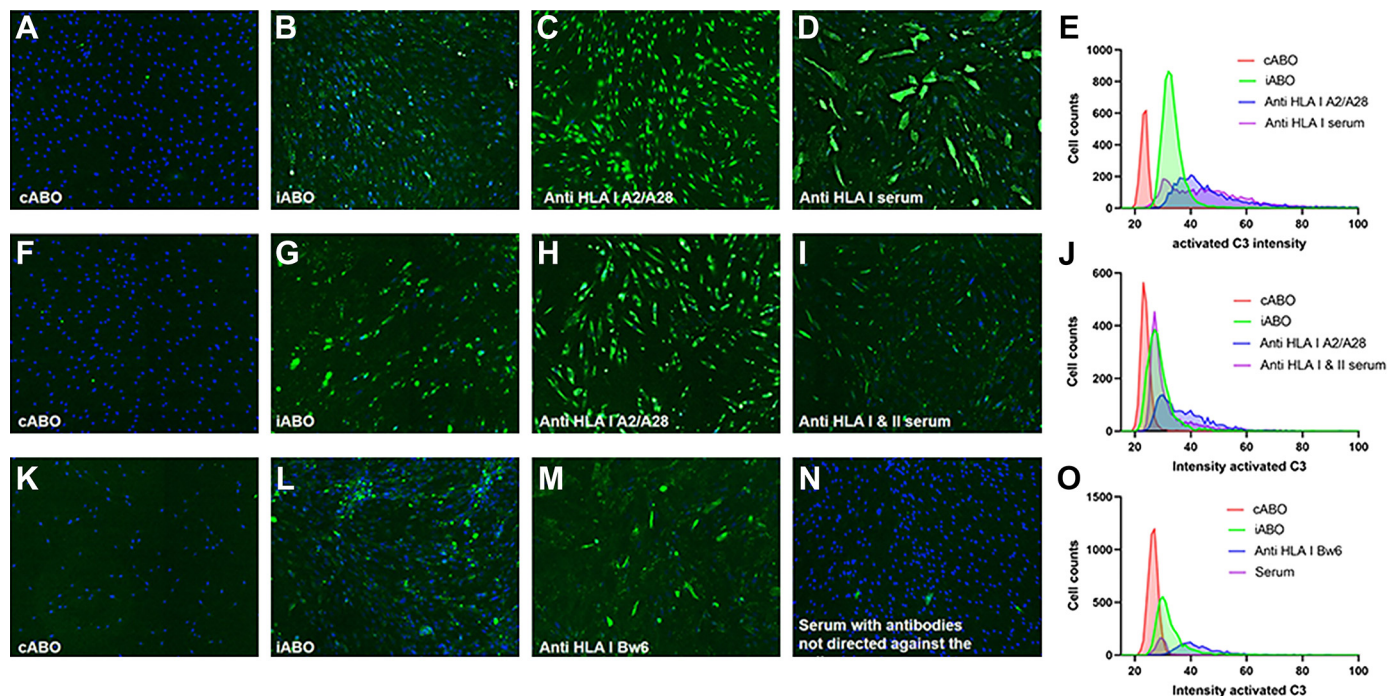
Figure 7. Antibody-mediated complement activation as shown by activated C3 staining on machine perfusion-derived primary renal endothelial cells (MP-PRECs) from three different donors. *A−E*: MP-PRECs with blood group A positive and human leukocyte antigen (HLA) typing A2 A19 A32 B7 B35 Bw6 Cw4 Cw7 DR2 DR15 DR6 DR13 DR51 DR52 DQ1 DQ1 DQ6 DQ6 incubated with blood group-compatible AB serum (cABO), blood group-incompatible O serum (iABO), a monoclonal human A2/A28 antibody, and serum with HLA class I and class II antibodies (A2, B17, B27, DR52, DR53, DR14, DR15, DR16, DQ5, DQ6, DQ12) directed against de HLA typing of the cell. *F−J*: MP-PRECs with blood group A-positive and HLA typing A2 A9 A23 B15 B62 B21 B49 Bw4 Bw6 Cw3 Cw7 DR4 DR5 DR11 DR52 DR53 DQ3 DQ3 DQ7 DQ8 DQ6 incubated with cABO, iABO, monoclonal human A2/A28 antibody, and serum with HLA class I and class II antibodies (A2, B17, B27, DR52, DR53, DR14, DR15, DR16, DQ5, DQ6, DQ12) directed against de HLA typing of the cell. *K − O*: MP-PRECs with blood group A-positive and HLA typing A9 A24 A28 A68 B7 B12 B44 Bw4 Bw6 Cw7 DR1 DR2 DR15 DR51 DQ1 DQ1 DQ5 DQ6 incubated with cABO, iABO, monoclonal human Bw6 antibody, and serum with HLA class II antibodies (DRB4, DR53) not directed against de HLA II typing of the cell. Magnification: ×10. In *E*, *J*, and *O*, histograms show quantification of the activated C3 staining. Results are expressed as mean fluorescence intensity of FITC staining in the green fluorescent protein channel.

relatively easily accessible source, by setting up a straightforward isolation technique. Immunological risk stratification still is a major challenge in organ transplantation (51). Complement fixing HLA antibodies as detected by the complement-dependent cytotoxicity test using donor lymphocytes as target cells will almost certainly lead to hyperacute rejection (51). However, HLA antibodies only detectable by the more sensitive bead-based Luminex assay are not an absolute barrier to transplantation but are associated with a variably increased risk of chronic antibody-mediated damage. To date, attempts to accurately predict the individual risk of poor outcomes in patients with DSA detected by the more sensitive bead assays have not been successful (52). DSA subclass analysis and the assays for complement-binding antibodies have not consistently improved the predictive capacity of current solid-phase assays (53). In addition, non-HLA antibodies are thought to contribute to graft loss in the absence of HLA antibodies (9, 54). However, the nature of these antibodies is still largely unknown, and no widely accepted assays exist to date. Non-HLA antibodies cannot be detected by the current lymphocyte-based complement-dependent cytotoxicity test. Therefore, MP-PRECs form an attractive basis for the development of assays to assess the pathogenicity of HLA antibodies and detect non-HLA antibodies against the renal endothelium. Numerous non-HLA antibodies have been reported in the past decade, of which

AGTR1 is one of the most established target antigens (9). Therefore, we investigated the gene expression of AGTR1 in MP-PRECs from four different donors and established the absence of expression in MP-PRECs (data not shown). This, together with the fact that Leisman et al. (55) recently showed that AGTR1 expression is mostly located at the site of mesangial and vascular smooth muscle cells, suggests that the endothelium does not express AGTR1 in the kidney.

As a proof of principle, we have shown in a cross-match assay using human monoclonal antibodies directed against the HLA typing of MP-PRECs but also with patient serum containing donor-specific antibodies and blood group-incompatible serum, that complement is activated on the cell membrane of MP-PRECs. Complement was activated to varying extents on different MP-PRECs, strengthening the current conception that characteristics of the target cell likely contribute to pathogenicity of donor-specific antibodies (20, 56).

We speculate that MP-PRECs could prove invaluable for studying immunological processes in renal allograft rejections and could lead to the development of new and highly required diagnostic tools (8, 9). In addition, after defining strict use (40), we suggest the use of the MP-PREC biobank as a rich source for creating immortalized renal EC lines, which differ in phenotype (e.g., microvascular vs. macrovascular; with or without the CD74 GB3 receptor, crucially

involved in HUS; blood groups and HLA alleles) and can be manipulated by, e.g., CRISPR/Cas technology.

In conclusion, we developed a technique to isolate and culture renal ECs from machine-perfused donor kidneys. The expression of EC markers varies between donors, which could be exploited to generate renal EC lines. These cells are a unique resource for studying complement (in)dependent cytotoxicity upon binding of donor-specific antibodies and for disease monitoring within the general population of patients with renal vasculopathic diseases.

APPENDIX A

Isolation of KA and Lifeport Transplant Perfusion Machine Perfusate Cells

Perfusate cell isolation was performed using sterile techniques in an enclosed flow cabinet that was cleaned using 70% ethanol.

The KA or Lifeport perfusion machine was collected from storage within 24 h after kidney perfusion (cold room 4°C) and placed in the enclosed flow cabinet. At the time of cell isolation, the outer part of the KA or Lifeport was no longer sterile, and therefore precautions were taken so as not to contaminate the perfusate cells contained inside. Using a 25-mL pipette, the perfusate fluid was resuspended inside the KA or Lifeport to ensure all cells were removed from surfaces inside the machine. The resuspended fluid was then transferred into two sterile 500-mL centrifuge tubes (Cat. No. CLS431123, Corning Sigma). Next, the perfusion machine filter of the Lifeport was unfastened, and the perfusate fluid retrogradely flushed out of the convoluted filter tubing into the main compartment of the perfusion machine and resuspended. This fluid was then also transferred into the 500-mL centrifuge tubes. Once completely emptied, the KA or Lifeport machine was removed, and the flow cabinet was resterilized using 70% ethanol.

Next, the 500-mL tubes were centrifuged [acceleration 7, deceleration 7, 4°C, 1,500 rpm (300 g)] for 15 min. The supernatant was then removed and disposed of, leaving a small amount of fluid in the tube. One-third of the cells were set aside for long-term storage. With the remaining cells, negative-based selection was performed by distributing the cells into uncoated T75 flasks, ensuring that all cells were transferred by rinsing the 500-mL flasks with culture medium (M200 culture medium, Ref. No. M200500, Gibco) supplemented with low growth serum (supplement kit, Ref. No. S-003-K, Gibco) and adding to the T75 flasks. Additional culture medium was added if necessary to ensure a total volume of 10 mL in the flasks. These flasks were then incubated at 37°C for 30–40 min. After the incubation period, cells were resuspended within the flasks. Nonadherent cells (containing ECs among other cell types) were cultured as described in APPENDIX B. The one-third of cells set aside for storage were centrifuged [1,000 rpm (200 g), 8 min, brake 8], and the supernatant was removed, leaving the cell pellet. Freeze medium (M200 cell culture medium with added 10% FBS and 10% DMSO, Ref. No. 109678, Merck) was added, resuspended with the cells, and transferred into a labeled ampule for freezing. The ampule containing the cells and freeze medium was then placed in Mr. Frosty at −80°C. The following day, the ampule was transferred to liquid nitrogen storage.

APPENDIX B

All cell cultivation and isolation techniques were performed using sterile techniques in an enclosed flow cabinet that was cleaned using 70% ethanol.

Cell Culture of Isolated ECs

Kidney transplant machine perfusate cells were isolated from kidney perfusion machines, and monocytes/macrophages were removed by plastic-based negative selection (see APPENDIX A) and cultivated as follows. Cells were seeded in two 1% sterile gelatin-coated T75 culture flasks in 12 mL cell culture medium composed of M200 culture medium (Ref. No. M200500, Gibco) supplemented with low growth serum (supplement kit, Ref. No. S-003-K, Gibco). The cell culture medium was exchanged every 2–3 days.

Isolation of ECs Using CD31 Immunomagnetic Beads Selection

CD31 immunomagnetic bead selection (Dynabeads CD31, Ref. No. 11155D, Invitrogen) of ECs was performed once cultured perfusate cells had reached confluent or almost confluent density.

CD31 immunomagnetic beads (400,000 beads/μL) and bead washing buffer, composed of Dulbecco's PBS [without Ca and Mg (Ref. No. BE17-512Q, LONZA)] and 0.1% sterile BSA solution (preparation: 10% BSA, Ref. No. A9647-100G, Sigma, diluted in Dulbecco's PBS using a 0.2-μm filter), were put on ice. Subsequently, trypsin-EDTA solution (Ref. No. R-001-100, Gibco), trypsin neutralizer solution (Ref. No. R-002-100, Gibco), and M200 culture medium (Ref. No. M200500, Gibco) supplemented with low growth serum (supplement kit, Ref. No. S-003-K, Gibco) were allowed to heat up to room temperature and then placed in a water bath at 37°C.

To begin isolation of cells, 2 μL of CD31 immunomagnetic beads were placed in a 1.5-mL sterile Eppendorf tube and washed (repeatedly resuspended) in 1 mL of bead washing buffer. The Eppendorf tube containing the CD31 beads-bead wash mix was then placed in a magnet for 2 min. After 2 min, the supernatant was carefully removed, leaving the CD31 beads in the tube. The CD31 beads were then resuspended in 80 μL of bead washing buffer to create the bead stock (10,000 beads/μL). This was then stored on ice.

Next, 1 μL of CD31 bead stock was then added to the T75 flask containing perfusate cells that had previously been in culture while keeping the cells in the medium. If the perfusate cells contained red blood cells, these were removed before adding the CD31 beads. The T75 flask containing perfusate cells and CD31 beads was then placed on a slow shaker for 10 min. After 10 min, cells were examined under a microscope to check if CD31 beads had attached (3–4 beads/cell is optimal). If there was insufficient CD31-bead attachment, the T75 flask was placed back on the slow shaker and the process of checking the mixing was repeated until the CD31 beads had attached.

Once attachment was sufficient, cells were collected as follows. Culture medium was removed and cells were washed twice: once with bead washing buffer and subsequently with PBS, both of which were at room temperature. Trypsin (2 mL) was then added to detach the cells from the flask. The flask was gently agitated, and 1.5 mL trypsin was instantly removed. This process was done at room temperature. Cells were then checked every 2 min under the microscope to assess detachment. Once cells were detached, 2 mL of trypsin neutralizer were added and resuspended. The end volume of cells and solution was then transferred to a 4.5-mL FACS tube.

To remove the cells with CD31-beads attached from the trypsin-trypsin neutralizer mixture, the 4.5-mL FACS tube was first placed in a magnet. CD31-bead cells moved to the side of the tube by the magnet. After 2 min, while in the magnet, the CD31-bead$^-$ cells and supernatant were removed carefully using a pipette, making sure not to disturb the CD31-bead$^+$ cells. CD31-bead$^-$ cells and the supernatant were placed in a 10-mL tube, centrifuged [1,000 rpm (200 g), 8 min] into a pellet, and the supernatant was removed and resuspended in culture medium. The procedure of CD31-bead attachment was then repeated on these cells to ensure all CD31$^+$ cells had the opportunity to become attached. CD31-bead$^-$ cells at this stage were re-seeded in a 1% sterile gelatin-coated T75 flask and cultured at 37°C.

Thereafter, the 4.5-mL tube with CD31-bead$^+$ cells was removed from the magnet, and 2.5 mL of cold bead washing buffer were pipetted down the back side of the tube (cell side), resuspended, and placed back into the magnet. After 2 min, the supernatant was carefully transferred into a 15-mL tube. This was classified as *washing step 1*. This was repeated until five washing steps were completed, each time placing the supernatant into the initial 15-mL tube. The appropriate cell culture vessel was chosen according to the estimated quantity of CD31$^+$ cells (60,000 cells/cm^2), coated with 1% sterile gelatin, and culture medium (according to Table A1) was added to the 4.5-mL tube and resuspended. Cells and medium were then transferred to the flask/plate and cultured at 37°C. Finally, the supernatant (containing cells) collected from each wash step in a 15-mL tube was centrifuged [1,000 rpm (200 g), 8 min] into a pellet, the supernatant was removed, and culture medium (according to Table A1) was added, resuspended, and plated into a culture flask/plate. These cells were cultured at 37°C.

Freezing of Confluent Cells

Once cells had become confluent, or when cells of interest needed to be stored long term, they were prepared for freezing as follows. Freeze-M200 (M200 cell culture medium with added 10% FBS (general MB) and 10% DMSO (Ref. No. 109678, Merck)] and a Mr. Frosty were precooled. Cells that were to be frozen were first washed twice using PBS. Cells were subsequently dethatched using trypsin. Trypsin was added to the cells containing the vesicle, agitated, detachment checked under a microscope, and, once detached, trypsin neutralizer was added (twice the volume of trypsin). Cells and trypsin-trypsin neutralizer supernatant were centrifuged [1,000 rpm (200 g), 8 min, brake 8], and the supernatant was removed, leaving the cell pellet. Freeze medium was added, resuspended with cells, and transferred into a labeled ampule for freezing. The ampule containing the cells and freeze medium was then placed in Mr. Frosty at −80°C. The following day, the ampule was transferred to liquid nitrogen storage.

DISCLAIMERS

The funder had no role in the design of the study; in the collection, analyses, or interpretation of data; in the writing of the manuscript, or in the decision to publish the results.

DISCLOSURES

No conflicts of interest, financial or otherwise, are declared by the authors.

AUTHOR CONTRIBUTIONS

R.G.M.L., L.M.L., J.v.d.B., and S.P.B. conceived and designed research; R.G.M.L., L.M.L., G.T., W.A.D., and H.L.L. performed experiments; R.G.M.L. and L.M.L. analyzed data; R.G.M.L., L.M.L., M.R.D., G.M., J.v.d.B., and S.P.B. interpreted results of experiments; R.G.M.L. prepared figures; R.G.M.L., G.M., J.v.d.B., and S.P.B. drafted manuscript; R.G.M.L., L.M.L., G.T., W.A.D., H.L.L., M.R.D., M.A.S., B.G.H., R.A.P. H.G.D.L., G.M., J.v.d.B., and S.P.B. edited and revised manuscript; R.G.M.L., M.R.D., H.G.D.L., G.M., J.v.d.B., S.P.B., and C.C. approved final version of manuscript.

Table A1. *Quantity of endothelial cell culture medium needed according to cell culture vessel*

Cell Culture Vessel	Quantity of Culture Medium, mL
T25 flask	4.0
6-well plate	1.5
12-well plate	0.8
24-well plate	0.5
48-well plate	0.3

REFERENCES

1. **Aird WC.** Phenotypic heterogeneity of the endothelium. I. Structure, function, and mechanisms. *Circ Res* 100: 158–173, 2007. doi:10.1161/01.RES.0000255691.76142.4a.

2. **Aird WC.** Phenotypic heterogeneity of the endothelium. II. Representative vascular beds. *Circ Res* 100: 174–190, 2007. doi:10.1161/01.RES.0000255690.03436.ae.

3. **Aird WC.** Endothelium in health and disease. *Pharmacol Rep* 60: 139–143, 2008. doi:10.1055/s-2007-1002703.

4. **Sengoelge G, Luo W, Fine D, Perschl AM, Fierlbeck W, Haririan A, Sorensson J, Rehman TU, Hauser P, Trevick JS, Kulak SC, Wegner B, Ballermann BJ.** A SAGE-based comparison between glomerular

and aortic endothelial cells. *Am J Physiol Renal Physiol* 288: F1290–F1300, 2005. doi:10.1152/ajprenal.00076.2004.

5. **Barry DM, McMillan EA, Kunar B, Lis R, Zhang T, Lu T, Daniel E, Yokoyama M, Gomez-Salinero JM, Sureshbabu A, Cleaver O, Di Lorenzo A, Choi ME, Xiang J, Redmond D, Rabbany SY, Muthukumar T, Rafii S.** Molecular determinants of nephron vascular specialization in the kidney. *Nat Commun* 10: 5705, 2019. doi:10.1038/s41467-019-12872-5.

6. **Dumas SJ, Meta E, Borri M, Goveia J, Rohlenova K, Conchinha NV, Falkenberg K, Teuwen L-A, de Rooij L, Kalucka J, Chen R, Khan S, Taverna F, Lu W, Parys M, De Legher C, Vinckier S, Karakach TK, Schoonjans L, Lin L, Bolund L, Dewerchin M, Eelen G, Rabelink TJ, Li X, Luo Y, Carmeliet P.** Single-cell RNA sequencing reveals renal endothelium heterogeneity and metabolic adaptation to water deprivation. *J Am Soc Nephrol* 31: 118–138, 2020. doi:10.1681/ASN.2019080832.

7. **Yan R, Van Meurs M, Popa ER, Li R, Zwiers PJ, Zijlstra JG, Moser J, Molema G.** Early heterogenic response of renal microvasculature to hemorrhagic shock/resuscitation and the influence of NF-κB pathway blockade. *Shock* 51: 200–212, 2019. doi:10.1097/SHK.0000000000001126.

8. **Thomas KA, Valenzuela NM, Reed EF.** The perfect storm: HLA antibodies, complement, FcγRs, and endothelium in transplant rejection. *Trends Mol Med* 21: 319–329, 2015. doi:10.1016/j.molmed.2015.02.004.

9. **Delville M, Lamarthée B, Pagie S, See SB, Rabant M, Burger C,** et al. Early acute microvascular kidney transplant rejection in the absence of anti-HLA antibodies is associated with preformed IgG antibodies against diverse glomerular endothelial cell antigens. *J Am Soc Nephrol* 30: 692–709, 2019. doi:10.1681/ASN.2018080868.

10. **Gupta G, Abu Jawdeh BG, Racusen LC, Bhasin B, Arend LJ, Trollinger B, Kraus E, Rabb H, Zachary AA, Montgomery RA, Alachkar N.** Late antibody-mediated rejection in renal allografts: outcome after conventional and novel therapies. *Transplantation* 97: 1240–1246, 2014. doi:10.1097/01.TP.0000442503.85766.91.

11. **Lefaucheur C, Loupy A, Vernerey D, Duong-Van-Huyen JP, Suberbielle C, Anglicheau D, Vérine J, Beuscart T, Nochy D, Bruneval P, Charron D, Delahousse M, Empana JP, Hill GS, Glotz D, Legendre C, Jouven X.** Antibody-mediated vascular rejection of kidney allografts: a population-based study. *Lancet* 381: 313–319, 2013. doi:10.1016/S0140-6736(12)61265-3.

12. **Loupy A, Haas M, Solez K, Racusen L, Glotz D, Seron D,** et al. The Banff 2015 kidney meeting report: current challenges in rejection classification and prospects for adopting molecular pathology. *Am J Transplant* 17: 28–41, 2017. doi:10.1111/ajt.14107.

13. **Bouïs D, Hospers GA, Meijer C, Molema G, Mulder NH.** Endothelium in vitro: a review of human vascular endothelial cell lines for blood vessel-related research. *Angiogenesis* 4: 91–102, 2001. doi:10.1023/A:1012259529167.

14. **French LE, Hahne M, Viard I, Radlgruber G, Zanone R, Becker K, Müller C, Tschopp J.** Fas and Fas ligand in embryos and adult mice: ligand expression in several immune-privileged tissues and coexpression in adult tissues characterized by apoptotic cell turnover. *J Cell Biol* 133: 335–343, 1996. doi:10.1083/jcb.133.2.335.

15. **Aird WC.** Endothelial cell heterogeneity. *Cold Spring Harb Perspect Med* 2: a006429, 2012. doi:10.1101/cshperspect.a006429.

16. **Molema G, Aird WC.** Vascular heterogeneity in the kidney. *Semin Nephrol* 32: 145–155, 2012. doi:10.1016/j.semnephrol.2012.02.001.

17. **Noris M, Galbusera M, Gastoldi S, Macor P, Banterla F, Bresin E, Tripodo C, Bettoni S, Donadelli R, Valoti E, Tedesco F, Amore A, Coppo R, Ruggenenti P, Gotti E, Remuzzi G.** Dynamics of complement activation in aHUS and how to monitor eculizumab therapy. *Blood* 124: 1715–1726, 2014. doi:10.1182/blood-2014-02-558296.

18. **Le Bas-Bernardet S, Hourmant M, Coupel S, Bignon J-D, Soulillou J-P, Charreau B.** Non-HLA-type endothelial cell reactive alloantibodies in pre-transplant sera of kidney recipients trigger apoptosis. *Am J Transplant* 3: 167–177, 2003. doi:10.1034/j.1600-6143.2003.00021.x.

19. **Satchell SCS, Tasman CHC, Singh A, Ni L, Geelen J, Von Ruhland CJ, O'Hare MJ, Saleem MA, Van Den Heuvel LPL, Mathieson PWP, O'hare M, Saleem MA, Van Den Heuvel LPL, Mathieson PWP.** Conditionally immortalized human glomerular endothelial cells expressing fenestrations in response to VEGF. *Kidney Int* 69: 1633–1640, 2006. doi:10.1038/sj.ki.5000277.

20. **Filippone EJ, Farber JL.** The humoral theory of transplantation: epitope analysis and the pathogenicity of HLA antibodies. *J Immunol Res* 2016: 5197396–5197312, 2016. doi:10.1155/2016/5197396.

21. **Organ Assist.** *Kidney-Assist Transport* [Online]. https://www.organ-assist.nl/products/kidney-assist__transport. Accessed 25 June 2020.

22. **Maathuis MHJ, Leuvenink HGD, Ploeg RJ.** Perspectives in organ preservation. *Transplantation* 83: 1289–1298, 2007. doi:10.1097/01.tp.0000265586.66475.cc.

23. **Delirezh N, Shojaeefar E, Parvin P, Asadi B.** Comparison the effects of two monocyte isolation methods, plastic adherence and magnetic activated cell sorting methods, on phagocytic activity of generated dendritic cells. *Cell J* 15: 218–223, 2013.

24. **Dayang E-Z, Plantinga J, ter Ellen B, van Meurs M, Molema G, Moser J.** Identification of LPS-activated endothelial subpopulations with distinct inflammatory phenotypes and regulatory signaling mechanisms. *Front Immunol* 10: 1–12, 2019. doi:10.3389/fimmu.2019.01169.

25. **Ivetic A.** A head-to-tail view of L-selectin and its impact on neutrophil behaviour. *Cell Tissue Res* 371: 437–453, 2018. doi:10.1007/s00441-017-2774-x.

26. **Eurotranplant Reference Laboratory.** *Eurotranplant Reference Laboratory* [Online]. https://www.etrl.org/. Accessed 25 June 2020.

27. **Human Protein Atlas**. *Human Protein Atlas/ENSG00000261371-PECAM1/tissue* [Online]. www.proteinatlas.org. Accessed 25 June 2020.

28. **Bhasin M, Yuan L, Keskin DB, Otu HH, Libermann TA, Oettgen P.** Bioinformatic identification and characterization of human endothelial cell-restricted genes. *BMC Genomics* 11: 342, 2010. doi:10.1186/1471-2164-11-342.

29. **Van Meurs M, Kurniati NF, Wulfert FM, Asgeirsdottir SA, De Graaf IA, Satchell SC, Mathieson PW, Jongman RM, Kümpers P, Zijlstra JG, Heeringa P, Molema G.** Shock-induced stress induces loss of microvascular endothelial Tie2 in the kidney which is not associated with reduced glomerular barrier function. *Am J Physiol Renal Physiol* 297: F272–F281, 2009. doi:10.1152/ajprenal.00137.2009.

30. **Pusztaszeri MP, Seelentag W, Bosman FT.** Immunohistochemical expression of endothelial markers CD31, CD34, von Willebrand factor, and Fli-1 in normal human tissues. *J Histochem Cytochem* 54: 385–395, 2006. doi:10.1369/jhc.4A6514.2005.

31. **Valentijn KM, Sadler JE, Valentijn JA, Voorberg J, Eikenboom J.** Functional architecture of Weibel-Palade bodies. *Blood* 117: 5033–5043, 2011. doi:10.1182/blood-2010-09-267492.

32. **Schrijvers BF, Flyvbjerg A, De Vriese AS.** The role of vascular endothelial growth factor (VEGF) in renal pathophysiology. *Kidney Int* 65: 2003–2017, 2004. doi:10.1111/j.1523-1755.2004.00621.x.

33. **Podgrabinska S, Braun P, Velasco P, Kloos B, Pepper MS, Jackson DG, Skobe M.** Molecular characterization of lymphatic endothelial cells. *Proc Natl Acad Sci USA* 99: 16069–16074, 2002 [Erratum in *Proc Natl Acad Sci USA* 100: 4970, 2003]. doi:10.1073/pnas.242401399.

34. **Ugorski M, Dziegiel P, Suchanski J.** Podoplanin—a small glycoprotein with many faces. *Am J Cancer Res* 6: 370–386, 2016.

35. **Breimer ME, Rydberg L, Jackson AM, Lucas DP, Zachary AA, Melancon JK, Von Visger J, Pelletier R, Saidman SL, Williams WW, Holgersson J, Tydén G, Klintmalm GK, Coultrup S, Sumitran-Holgersson S, Grufman P.** Multicenter evaluation of a novel endothelial cell crossmatch test in kidney transplantation. *Transplantation* 87: 549–556, 2009. doi:10.1097/TP.0b013e3181949d4e.

36. **Ligresti G, Nagao RJ, Xue J, Choi YJ, Xu J, Ren S, Aburatani T, Anderson SK, MacDonald JW, Bammler TK, Schwartz SM, Muczynski KA, Duffield JS, Himmelfarb J, Zheng Y.** A novel three-dimensional human peritubular microvascular system. *J Am Soc Nephrol* 27: 2370–2381, 2016. doi:10.1681/ASN.2015070747.

37. **Muczynski KA, Cotner T, Anderson SK.** Unusual expression of human lymphocyte antigen class II in normal renal microvascular endothelium. *Kidney Int* 59: 488–497, 2001. doi:10.1046/j.1523-1755.2001.059002488.x.

38. **Moers C, Smits JM, Maathuis M-HJ, Treckmann J, van Gelder F, Napieralski BP, van Kasterop-Kutz M, van der Heide JJH, Squifflet J-P, van Heurn E, Kirste GR, Rahmel A, Leuvenink HGD, Paul A, Pirenne J, Ploeg RJ.** Machine perfusion or cold storage in deceased-donor kidney transplantation. *N Engl J Med* 360: 7–19, 2009. doi:10.1056/NEJMoa0802289.

39. **Lorsch BJR**, **Collins FS**, **Lippincott-Schwartz J.** Fixing problems with cell lines: technologies and policies can improve authentication. *Science* 346: 1452–1453, 2014. doi:10.1126/science.1259110.

40. **Cleuren ACA**, **van der Ent MA**, **Jiang H**, **Hunker KL**, **Yee A**, **Siemieniak DR**, **Molema G**, **Aird WC**, **Ganesh SK**, **Ginsburg D.** The in vivo endothelial cell translatome is highly heterogeneous across vascular beds. *Proc Natl Acad Sci USA* 116: 23618–23624, 2019. doi:10.1073/pnas.1912409116.

41. **Tsvetkov D**, **Kolpakov E**, **Kassmann M**, **Schubert R**, **Gollasch M.** Distinguishing between biological and technical replicates in hypertension research on isolated arteries. *Front Med* 6: 1–8, 2019. doi:10.3389/fmed.2019.00126.

42. **Haudenschild CC**, **Cotran RS**, **Gimbrone MA**, **Folkman J.** Fine structure of vascular endothelium in culture. *J Ultrastruct Res* 50: 22–32, 1975. doi:10.1016/s0022-5320(75)90004-0.

43. **Nachman RL**, **Jaffe EA.** Endothelial cell culture: beginnings of modern vascular biology. *J Clin Invest* 114: 1037–1040, 2004. doi:10.1172/JCI200423284.

44. **Malek M**, **Nematbakhsh M.** Renal ischemia/reperfusion injury; from pathophysiology to treatment. *J Renal Inj Prev* 4: 20–207, 2015. doi:10.12861/jrip.2015.06.

45. **Welbourn CRB**, **Goldman G**, **Paterson IS**, **Valeri CR**, **Shepro D**, **Hechtman HB.** Pathophysiology of ischaemia reperfusion injury: central role of the neutrophil. *Br J Surg* 78: 651–655, 1991. doi:10.1002/bjs.1800780607.

46. **Sol M**, **Kamps JAAM**, **van den Born J**, **van den Heuvel MC**, **van der Vlag J**, **Krenning G**, **Hillebrands JL.** Glomerular endothelial cells as instigators of glomerular sclerotic diseases. *Front Pharmacol* 11: 1–13, 2020. doi:10.3389/fphar.2020.573557.

47. **Snoeijs MG**, **Vink H**, **Voesten N**, **Christiaans MH**, **Daemen JWH**, **Peppelenbosch AG**, **Tordoir JH**, **Peutz-Kootstra CJ**, **Buurman WA**, **Schurink GWH**, **Van Heurn LWE.** Acute ischemic injury to the renal microvasculature in human kidney transplantation. *Am J Physiol Renal Physiol* 299: F1134–F1140, 2010. doi:10.1152/ajprenal.00158.2010.

48. **Muczynski KA**, **Ekle DM**, **Coder DM**, **Anderson SK.** Normal human kidney HLA-DR-expressing renal microvascular endothelial cells: characterization, isolation, and regulation of MHC class II expression. *J Am Soc Nephrol* 14: 1336–1348, 2003. doi:10.1097/01.asn.0000061778.08085.9f.

49. **Kurniati NF**, **Jongman RM**, **Vom Hagen F**, **Spokes KC**, **Moser J**, **Regan ER**, **Krenning G**, **Moonen JRAJ**, **Harmsen MC**, **Struys MMRF**, **Hammes HP**, **Zijlstra JG**, **Aird WC**, **Heeringa P**, **Molema G**, **Van Meurs M.** The flow dependency of Tie2 expression in endotoxemia. *Intensive Care Med* 39: 1262–1271, 2013. doi:10.1007/s00134-013-2899-7.

50. **Olarerin-George AO**, **Hogenesch JB.** Assessing the prevalence of mycoplasma contamination in cell culture via a survey of NCBI's RNA-seq archive. *Nucleic Acids Res* 43: 2535–2542, 2015. doi:10.1093/nar/gkv136.

51. **Patel R**, **Terasaki PI.** Significance of the positive crossmatch test in kidney transplantation. *N Engl J Med* 280: 735–739, 1969. doi:10.1056/NEJM196904032801401.

52. **Kamburova EG**, **Wisse BW**, **Joosten I**, **Allebes WA**, **van der Meer A**, **Hilbrands LB**, et al. Differential effects of donor-specific HLA antibodies in living versus deceased donor transplant. *Am J Transplant* 18: 2274–2284, 2018. doi:10.1111/ajt.14709.

53. **Loupy A**, **Lefaucheur C**, **Vernerey D**, **Prugger C**, **van Huyen J-PD**, **Mooney N**, **Suberbielle C**, **Frémeaux-Bacchi V**, **Méjean A**, **Desgrandchamps F**, **Anglicheau D**, **Nochy D**, **Charron D**, **Empana J-P**, **Delahousse M**, **Legendre C**, **Glotz D**, **Hill GS**, **Zeevi A**, **Jouven X.** Complement-binding anti-HLA antibodies and kidney-allograft survival. *N Engl J Med* 369: 1215–1226, 2013. doi:10.1056/NEJMoa1302506.

54. **Delville M**, **Charreau B**, **Rabant M**, **Legendre C**, **Anglicheau D.** Pathogenesis of non-HLA antibodies in solid organ transplantation: where do we stand? *Hum Immunol* 77: 1055–1062, 2016. doi:10.1016/j.humimm.2016.05.021.

55. **Leisman DE**, **Fernandes TD**, **Bijol V**, **Abraham MN**, **Lehman JR**, **Taylor MD**, **Capone C**, **Yaipan O**, **Bellomo R**, **Deutschman CS.** Impaired angiotensin II type 1 receptor signaling contributes to sepsis-induced acute kidney injury. *Kidney Int* 99: 148–160, 2021. doi:10.1016/j.kint.2020.07.047.

56. **Lim WH**, **Wong G**, **Heidt S**, **Claas FHJ.** Novel aspects of epitope matching and practical application in kidney transplantation. *Kidney Int* 93: 314–324, 2018. doi:10.1016/j.kint.2017.08.008.